THE ASTROPHYSICAL JOURNAL, 449:86–92, 1995 August 10

PAIR CASCADES IN EXTRAGALACTIC JETS. II. THE BEAMED X-RAY SPECTRUM

AMIR LEVINSON AND ROGER BLANDFORD
Theoretical Astrophysics, 130-33 Caltech, Pasadena, CA 91125
Received 1994 November 30; accepted 1995 February 21

ABSTRACT

The X-ray through γ-ray emission from a relativistic jet is considered within the framework of an inhomogeneous pair-cascade model. It is shown that the overall spectrum from the model exhibits a spectral break at an energy of order $(m_e c^2)^2/E_b$, where E_b is the cutoff energy of the isotropic spectrum of scattered X-ray photons, above which the γ-rays are subject to significant absorption through pair production on the ambient soft radiation. Such a break has been observed thus far in the γ-ray spectra of several blazars; if blazars possess isotropic X-ray spectra similar to those observed in radio-quiet sources, then the relation between the break energy and the cutoff energy, predicted by our model, is roughly satisfied. It is argued that emission just below the γ-ray break originates near the base of the jet and is determined by the distribution function of cascading pairs there. Above the break, the slope of the emergent γ-ray spectrum reflects the radial variations of pair acceleration and soft photon intensity and should be steeper than the hard X-ray spectrum. For plausible particle acceleration prescriptions and soft radiation spectra, the characteristic hard X-ray spectra observed in some blazars are reproduced by our model. The X-ray cutoff energy is also related to the dynamics of the jet. It is argued that both the inertia and the radiative drag acting upon a jet increase sharply when the bulk Lorentz factor exceeds $\Gamma_c \sim (m_e c^2/E_b) \sim 10$ and that jets will be accelerated up to this critical Lorentz factor which is of order that inferred from VLBI observations of superluminal radio sources. The utility of multiwaveband observations for advancing our understanding of blazars is stressed.

Subject headings: galaxies: jets — gamma rays: theory — X-rays: galaxies

1. INTRODUCTION

The detection of bright, variable γ-ray emission from blazars by the EGRET instrument on the *Compton Gamma Ray Observatory* (*CGRO*) provides additional support to the unified model for active galactic nuclei (AGNs). About 40 blazars, and no radio-quiet AGNs or extended radio sources, have been reported thus far as >100 MeV γ-ray sources (Kurfess et al. 1994; Thompson et al. 1994). The γ-ray emission is presumably beamed and originates deep within a relativistic jet. Five of the EGRET AGN sources have also been detected by the COMPTEL instrument at energies above a few MeV (Collmar et al. 1993, 1994; Blom et al. 1994; Lichti et al. 1994). The combined COMPTEL and EGRET data indicate spectral breaks (or curvature) at energies between 1 and 30 MeV, with softening of the spectrum above the break. In the case of the quasar 3C 273, which has been observed simultaneously by different instruments over a large range of frequencies (Lichti et al. 1994), the combined *Ginga*, BATSE, OSSE, COMPTEL, and EGRET data suggest a spectral steepening by ~ 0.8 at an energy ~ 1.5 MeV.

Many quasars also exhibit an opposite spectral break at soft X-ray energies (typically at 1–2 keV). The extreme UV through soft X-ray spectrum (below ~ 1 keV) is consistent with a power law with spectral index $\gtrsim 1.5$. The hard X-ray spectra appear to be flatter with spectral indices in the range $\alpha_x = 0.5$–0.8 for radio-loud quasars, and $\alpha_x \gtrsim 1$ for radio-quiet quasars and BL Lac objects (e.g., Wilkes & Elvis 1987; Brunner et al. 1994; Laor et al. 1994). Whereas the hard X-ray emission observed in radio-quiet quasars is most likely isotropic, the hard X-ray flux seen from blazars is probably dominated by a beamed component which is produced in the jet. The soft X-ray (sub-keV) spectrum of quasars is commonly interpreted as the high energy extension of the "blue bump." In a previous paper (Blandford & Levinson 1995, hereafter Paper I) we have described an inhomogeneous pair cascade model, proposed originally by Blandford (1993), for the γ-ray emission from blazars observed by EGRET. A brief summary of the model and the results obtained in Paper I are given in § 2.1. We then go on to generalize the pair cascade model to incorporate hard X-ray emission and compute spectra in the energy range encompassing the hard X-ray through the EGRET range. We find that the hard X-ray spectrum is produced predominantly by inverse Compton scattering at the smallest jet radii and reflects the local pair cascade spectrum, which in turn depends on the spectrum of the reprocessed ultraviolet soft X-ray (UVX) radiation. In contrast, the γ-ray spectrum above $(m_e c^2/E_b)$, where E_b is the cutoff energy of the soft radiation spectrum (henceforth we measure all energies implicitly in units of $m_e c^2$), depends on the radial variations of soft-photon intensity and particle acceleration and is steeper than the hard X-ray spectrum. Thus, the spectral break at soft γ-ray energies $(\sim m_e c^2/E_b)$ arises quite naturally in the pair cascade model.

In § 3, we turn to the dynamical implications of this model and argue that the radiative drag on a jet increases rapidly after the bulk Lorentz factor Γ exceeds $\Gamma_c = (m_e c^2/E_b)$ so that cooled electron-positron pairs can create additional pairs on the ambient radiation field.

A version of the inhomogeneous pair-cascade model has been proposed earlier by Burns & Lovelace (1982). The physics of homogeneous pair-photon cascades has been considered by Svensson (1987) and Zdziarski (1988), who applied their models to the X-ray emission from Seyfert galaxies. Several other models for the beamed X- and γ-ray emission from jets, involving inverse Compton scattering by accelerated particles, have also been proposed previously. Inhomogeneous synchrotron self-Compton models (e.g., Königl 1981; Ghisellini & Maraschi 1989; Bloom & Marscher 1993) seem difficult to fit to the spectra observed from powerful blazars (Paper I)

but may be applicable to low-power BL Lac objects. The comparison with other models (e.g., Melia & Königl 1989; Dermer & Schlickeiser 1993; Sikora, Begelman, & Rees 1994) is also discussed in Paper I. The extension of these ideas to encompass synchrotron emission at lower frequency will be discussed in Paper III (Levinson 1995).

2. X- AND γ-RAY EMISSION FROM RELATIVISTIC JETS

2.1. *Summary of the γ-Ray Jet Model Presented in Paper I*

A key feature of the pair cascade model presented in Paper I is that the observed γ-ray spectrum is a superposition of spectra produced over a large range of jet radii, with higher energy photons produced at larger radii. The γ-ray emission observed is predominantly due to inverse Compton scattering of ambient soft photons by relativistic pairs accelerated to high energies (in excess of the EGRET energy range) by shock fronts in a relativistic jet. At small jet radii, the γ-rays thereby created are severely attenuated by pair production on the soft photons; the observed γ-rays, at a given energy, E_γ, must therefore originate from close to a radius [$r_\gamma(E_\lambda)$, the *γ-spheric radius*] beyond which the opacity to pair production is less than unity. This γ-spheric radius increases with increasing γ-ray energy. The injection of pairs, at a given radius, to energies well above the associated threshold energy at which the pair-production opacity is unity, results in the development of a cascade down to energies at which the γ-rays can escape freely to infinity. The slope of the emergent γ-ray spectrum is determined by the spectrum and radial variation of the ambient soft radiation and by the pair injection rate. However, it is highly insensitive to the spectrum of injected pairs, provided that the efficiency of pair acceleration is sufficiently high, namely that pairs injected at energies $\gtrsim 10$ GeV carry a significant fraction of the power dissipated in the jet. The emergent γ-ray spectra, calculated numerically in Paper I, are in good agreement with observed EGRET spectra. The efficiency with which energy is converted from injected pairs to EGRET γ-rays is typically high and could exceed 50% in some cases.

Three different models for the distribution of soft photons were considered in Paper I: UVX photons that are coming from the central source and Thomson scattered across the jet by some material surrounding the jet, soft radiation scattered by an equatorial disk, and beamed radiation. For each of these sources we computed the γ-spheric radius and found it to be in the range 10^{15}–10^{18} cm, depending on γ-ray energy, soft radiation spectrum, and overall AGN luminosity. We also introduced the notion of the *annihilation radius* within which the pair density is limited by annihilation, and the *inner jet*, $r < r_{\rm ann}$, where, we argued, some additional carrier of momentum to electron-positron pairs must be present. Below the annihilation radius the pairs can cool to subrelativistic energies on a dynamical timescale, and pair annihilation becomes important and limits the pair density. The power carried by the pairs in the inner jet can be easily estimated and has been shown to be significantly smaller than the inferred power in γ-rays. It has been concluded, therefore, that there must be some other carrier of energy and momentum at small scales. Some possibilities were discussed in Paper 1.

2.2. *Rate of Beamed X-Ray Production by Inverse Compton Scattering*

We consider X-ray emission produced by inverse Compton scattering of soft radiation by relativistic pairs accelerated in a jet with a given bulk Lorentz factor Γ and which also produce the EGRET spectrum. We assume that the pairs are distributed isotropically in the comoving frame and denote by $N_e(E_e, r)$ their number density per unit log energy per unit jet radius (in what follows, subscripts "e," "γ," "x," and "s" refer to pairs, γ-rays, beamed X-rays, and soft photons, respectively). We also assume that the soft-photon distribution is isotropic in the AGN frame. As viewed from the comoving frame, the soft radiation is beamed along the direction pointing toward the central source and blueshifted by a factor of order Γ. Moreover, a power-law spectrum, $\tilde{I}_s(r, E_s) = \tilde{I}_o(r)(E_s)^{-\alpha}$; $E_a < E_s < E_b$, is transformed into a power-law spectrum with the same spectral index in the range $\Gamma E_a < E_s < \Gamma E_b$ (Paper I). The soft-photon intensity in the comoving frame can then be approximated as: $\tilde{I}_s(r, \mu, E_s) = \tilde{I}_s(r, E_s)\delta(1 + \mu)$ (Paper I).

Let us denote by $N_x(E_x, r)$ the angle-averaged number density per unit log energy per unit radius of the beamed hard X-rays. The evolution of N_x in the comoving frame is governed by the equation

$$\Gamma \frac{dN_x(E_x, r)}{d\ln r} = \zeta \int d\ln E_e\, \tilde{\eta}_{cx}(E_e, E_x) N_e(E_e)\,, \qquad (2.1)$$

where ζ depends on the angular distribution of the beamed radiation in the comoving frame and is of order unity, and $\tilde{\eta}_{cx}(E_e, E_x)$ is the angle-averaged Compton redistribution function. To first order in E_x/E_a the Compton redistribution function takes the form (Paper I)

$$\tilde{\eta}_{cx}(E_x, \mu; E_e) = \frac{E_x}{4\beta E_e(E_e - E_x)} \int_{\ln E_s}^{\ln E_b} E_s^{-1} \tilde{I}_s(E_s) d\ln E_s\,, \qquad (2.2)$$

where

$$\tilde{E}_s = \begin{cases} \dfrac{(1-\beta)E_e E_x}{(1-\beta\mu)E_e - (1-\mu)E_x} & \mu_o < \mu\,, \\ E_a & -1 \le \mu < \mu_o\,, \end{cases}$$

with

$$\mu_o = 1 - \frac{(1-\beta)(E_x/E_a - 1)}{\beta - E_x/E_e} \simeq 1 - \frac{E_x}{2E_a E_e(E_e - E_x)}\,,$$

and $\beta = (1 - E_e^{-2})^{1/2}$. For a power-law soft-photon intensity, $\tilde{I} \propto (E_s)^{-\alpha}$, the angle-averaged redistribution function can be easily computed. One finds

$$\tilde{\eta}_{cx}(E_x, E_e) = \frac{(\alpha+1)^{-1}\tilde{I}_o E_x^{-\alpha}}{4E_e - E_x} \times \begin{cases} \left(\dfrac{E_x}{E_a}\right)^{\alpha+1}\left[2 - \dfrac{(a+1)[2(\alpha+2)]^{-1}}{E_e(E_e - E_x)}\left(\dfrac{E_x}{E_a}\right)\right] & E_o < E_e \le E_{\rm max} \\ \dfrac{2^{2\alpha+3}}{\alpha+2}\,[E_e(E_e - E_x)]^{\alpha+1} & E_{\rm min} \le E_e < E_o \end{cases} \qquad (2.3)$$

Here $E_o = E_x/2 + (E_x^2 + E_x/E_a)^{1/2}/2$, and $E_{\rm min}$ and $E_{\rm max}$ are the low- and high-energy cutoffs of the pair spectrum. For a soft photon spectrum which consists of superposition of power-law spectra, the redistribution function can be obtained in a similar manner. To find the spectrum of the beamed hard X-rays, we must specify the pair cascade spectrum. For illustrative purposes we consider a power-law pair spectrum, $N_e(E_e) = N_o(E_e)^{-(p-1)}$; $E_{\rm min} \le E_e \le E_{\rm max}$. One then finds, using equations (2.1) and (2.3), that the hard X-ray intensity is, to a good approximation, a power law with index $\alpha_x = (p-1)/2$ for

$p < 2\alpha + 1$, and $\alpha_x = \alpha$ for $p > 2\alpha + 1$. This result is readily understood; for given E_e and E_x the energy of the scattered soft photon is approximately $E_s \simeq E_e^{-2} E_x$. For the power-law soft-photon intensity given above, the emissivity is then proportional to $E_e^{2\alpha} E_x^{-\alpha}$, as also clearly seen from equation (2.3). Thus, if the slope of the pair spectrum is steeper than $2\alpha + 1$, the production of X-rays at energy E_x is predominantly due to scattering of soft photons of energy $E_s \simeq E_x E_{\min}^2$ by pairs having energies near $E_{\min}$, in which case the X-ray spectrum reflects the spectrum of the soft radiation. In the opposite case, $p < 2\alpha + 1$, the X-ray production rate at E_x is dominated by scattering of photons having energies near E_a by pairs with energy $E_e \simeq (E_x/E_a)^{1/2}$ and consequently, the slope of the X-ray spectrum is $(p - 1)/2$. (It should be noted that if the pair spectrum has a low-energy cutoff at $E_{\min} \gg 1$, then the X-ray spectrum breaks at energy $E_a E_{\min}^2$ below which it is a power law with index $\alpha_x = 1$. For the pair cascade model discussed here, $E_{\min} \simeq 1$.) As we shall show below, the pair cascade spectrum is not a strict power law and moreover, it evolves with jet radius. Nevertheless, this simple example demonstrates that the hard X-ray spectrum is insensitive to the details of the cascade evolution and depends only weakly on the spectrum of soft photons (provided that pair acceleration is sufficiently efficient) through the distribution of cascading pairs at small radii, as will be verified below.

2.3. *Numerical Results*

The development of the pair cascade spectrum along the jet has been modeled in Paper I by solving numerically a set of kinetic equations describing the evolution of the angle-averaged pair and γ-ray number densities in the energy range 100 MeV to >10 GeV. The processes included are Compton scattering of ambient soft photons, pair creation and annihilation, and pair acceleration. The pair distribution is supposed to be isotropic in the comoving frame. The computations were performed in the comoving frame, and the intensities in the AGN frame were then obtained by appropriate Lorentz transformations. The comoving pair injection rate per unit log energy per unit radius is assumed to take the form $\tilde{S}(E_e, r) = f(E_e)(r/r_o)^{-(p+1)}$, where $f(E_e)$ is the spectrum of injected pairs, and the soft photon intensity has the form $\tilde{I} = g(E_s)(r/r_o)^{-(q+1)}$. The standard soft radiation spectrum is defined as

$$g(E_e) = K\left(\frac{E_s}{10^{-3}}\right)^{-0.5}\left[1 + \left(\frac{E_s}{10^{-3}}\right)^{-1}\right], \quad 10^{-5} < E_s < 10^{-1},$$

with $K = 10$. In what follows, we adopt the same notation. We emphasize that this form of the intensity is obtained in Paper I, assuming that the source of soft photons is Thomson scattering of nuclear radiation across the jet by some ambient ionized gas. However, at the small radii at which the hard X- and soft γ-rays are produced, radiation coming directly from the disk may provide an additional source of soft photons (Dermer & Schlickeiser 1993), and this may alter the soft photon intensity. Nevertheless, to explore the general properties of the emitted X-ray spectrum, it is sufficient to employ simple forms of soft photon intensity. As discussed in Paper I, a complete treatment of the jet bulk dynamic requires additional physics. The prescription adopted in Paper I and in this paper is that the jet width and Lorentz factor are constant (thereby neglecting adiabatic losses due to expansion of the jet). In addition to specifying the soft radiation spectrum, we must also specify the bulk Lorentz factor Γ.

We have extended the model of Paper I to include beamed X-ray emission. Specifically, we added equation (2.1), which describes the evolution of the X-ray spectrum, to the system of equations which govern the evolution of the pair and >5 MeV γ-ray number densities (eqs. [4.5] and [4.6] of Paper I) and integrated the coupled system, starting from some fiducial radius below the γ-spheric radius at a few MeV as measured in the comoving frame. The boundary condition imposed in the examples presented below is $N_e = N_\gamma = N_x = 0$. It is found, however, that the emergent spectra are highly insensitive to boundary conditions, as expected.

We find that as long as the injected energy spectrum is flatter than about $E_e^{-1.5}$, the pair cascade spectra at the base of the γ-ray jet, where most of the hard X-ray flux is produced, are power laws with index ~ 1.7–1.8, independent of the injected spectrum. When the energy spectrum of injected pairs becomes steeper than about 1.5, the pair cascade spectrum reflects the injected spectrum and is slightly softer than it.

Sample photon and pair spectra in the energy range 10 keV to 10 GeV, as measured in the AGN frame, are shown in Figures 1–3, for $\Gamma = 10$. Figures 1 and 2 show the development of the pair and the corresponding photon spectra down the jet, respectively. The four spectra plotted in each window were obtained at radii $r = 1.1$, 3, 30, and 3×10^4 in units of the γ-spheric radius at a γ-ray energy of 2 MeV, measured in the comoving frame (or, equivalently, $E_\gamma \sim 20$ MeV measured in the AGN frame), with larger radii corresponding to larger number densities, as indicated for example in Figure 1*a*. The spectra were all computed using the standard soft spectrum with $q = 0$ (Figs. 1*a*–1*c* and 2*a*–2*c*) and $q = 1$ (Figs. 1*d* and 2*d*), and pair source function with $p = -1$ (Figs. 1*a*–1*b* and 2*a*–2*b*) and $p = 0$ (Figs. 1*c*–1*d* and 2*c*–2*d*). The spectrum of injected pairs is taken to be $f(E_e) \propto \delta(E_e - E_{\max})$, with $E_{\max} = 5$ GeV in Figures 1*a*, 1*c*, 1*d*, 2*a*, 2*c*, and 2*d*, and $f(E_e) \propto E_e^{-1}$ in Figures 1*b* and 2*b*. As seen from Figure 1, there are no remarkable differences between the pair spectra at sufficiently large depths and most importantly, the pair cascade spectrum is insensitive to the injected spectrum. Consequently, the slope of the hard X-ray spectrum below E_b^{-1} ($E_b = 0.1$ in this example), which is produced predominantly at small radii, shows no evolution with radius and is insensitive to the details of injection and radial variations of soft-photon intensity. In contrast, the γ-ray spectrum above E_b^{-1} evolves significantly with radius (except for the case shown in Figs. 1*c* and 2*c* which corresponds to the self-similar solution discussed in Paper I), due to the dependence of γ-spheric radius on γ-ray energy, and the emergent spectrum reflects the spectrum and radial variations of pair injection rate and soft photon intensity (Paper I). As a result, the overall spectrum exhibits a spectral break at around E_b^{-1}. This might explain the spectral break observed in several blazars at soft γ-ray energies discussed in the introduction. The sharp spectral break obtained in this example reflects the sharp cutoff in the isotropic X-ray spectrum assumed. We find that a smooth high-energy turnover in the isotropic spectrum rather than a sharp cutoff results in smearing of the spectral break. As seen from Figure 2, the X-ray spectra are power laws with spectral indices in the range 0.75–0.65, in rough agreement with observations.

In Figure 3 we plotted emergent photon spectra, normalized to the total energy injected $\int \tilde{S}(E_e) dE_e\, dr$, for different soft radiation spectra and pair source function. In all cases $p = -1$ and $q = 0$. The spectra exhibited in the upper panel were calculated using $f(E_e) = \delta(E_e - E_{\max})$ but different soft photon intensities: standard soft radiation spectrum (*solid line*), $g(E_s) \propto E_s^{-1.5}$

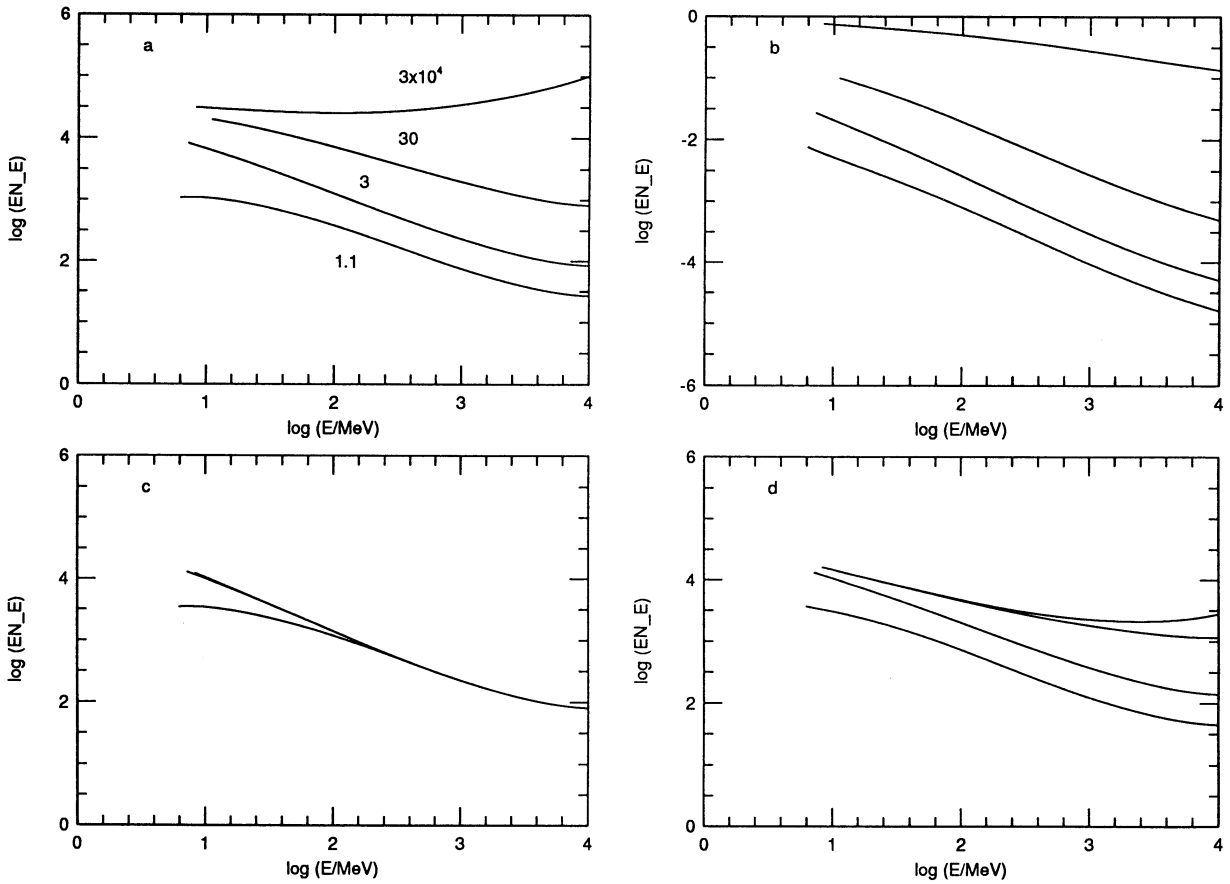

FIG. 1.—Local pair spectra exhibited as spectral efficiencies with arbitrary normalization. All spectra were obtained using the standard soft-photon spectrum with: (*a*) $q = 0$, $p = -1$; (*b*) $q = 0$, $p = -1$, $f(E_e) \propto E_e^{-1}$; (*c*) $q = 0$, $p = 0$; and (*d*) $q = 1$, $p = 0$. In cases (*a*), (*c*), and (*d*), $f(E_e) \propto \delta(E_e - E_{max})$, with $E_{max} = 5$ GeV as measured in the comoving frame. The four curves in each window correspond to $r = 1.1, 3, 30, 3 \times 10^4$ [labels the curves in (*a*)], where r is the jet radius in units of the γ-spheric radius at 2 MeV, and they show the development of the pair cascade spectrum with radius.

(*dotted line*), and $g(E_s) \propto E_s^{-0.5}$ (*dashed line*). As seen, the slope of the beamed X-ray spectrum depends on the extreme UV spectrum but is insensitive to changes in the hard X-ray portion of the ambient radiation spectrum, though steeper ambient X-ray spectra give rise to smoother turnover of the γ-ray spectrum. The spectrum of the beamed X-rays hardens slightly with flattening of the soft-radiation spectrum. The reason is that, as the soft-radiation spectrum becomes flatter, the Compton cooling rate increases slower with E_e, thereby giving rise to a harder pair cascade spectrum and hence, harder X-ray spectrum. The bottom panel presents spectra obtained for standard soft-photon spectrum and different source functions with injection spectra of the form $f(E_e) \propto E_e^{\delta}$ (δ labels the curves). This example indicates that the hard X-ray spectrum is independent of the spectrum of injected pairs provided that it is flatter than about -1.5. When the injected spectrum becomes very steep, the beamed X-ray spectrum reflects the spectrum of the ambient soft radiation (but is slightly harder than it), as expected from the simple analytic analysis of the previous subsection.

3. DYNAMICAL IMPLICATIONS

In the previous section we demonstrated how the hypothesis that compact radio sources contain, in addition to relativistic jets, an isotropic source of X-rays with similar spectral shape to that directly observed in the case of Seyfert galaxies, led to γ-ray spectra similar to those observed. We carried out these calculations assuming a specific, fixed value for the bulk Lorentz factor Γ. It turns out that there is a second implication of this hypothesis, namely, that the favored bulk Lorentz factor for the asymptotic jet speed will lie in the range $3 \lesssim \Gamma \lesssim 30$, as inferred from observations of superluminal expansion (e.g., Vermeulen & Cohen 1994) and statistical analyses of beaming fractions (e.g., Orr & Browne 1982).

In Paper I, we outlined a general jet model in which energy is extracted from a spinning black hole by an externally supported electromagnetic field and collimated by a surrounding hydromagnetic wind. Initially, the energy and momentum flux in the jet are carried by electromagnetic fields as a Poynting flux. However, as the jet propagates away from the central black hole, there is a steady conversion of electromagnetic energy into energy carried by electrons and positrons, in a manner reminiscent of models of pulsar winds (e.g., Kennel & Coroniti 1984). The transition from electromagnetic to particle dominance was seen to occur in the vicinity of the annihilation radius at the end of the inner jet. The rate of pair annihilation increases as the relative velocity of the particles becomes subrelativistic. It will generally be the case that electrons can cool to mildly relativistic energy in the comoving frame within r_{ann}. They will therefore mostly have energies $\sim\Gamma$ when measured in the AGN frame. Now suppose that the isotropic spectrum of soft X-rays cuts off near E_b, and suppose also that the bulk flow

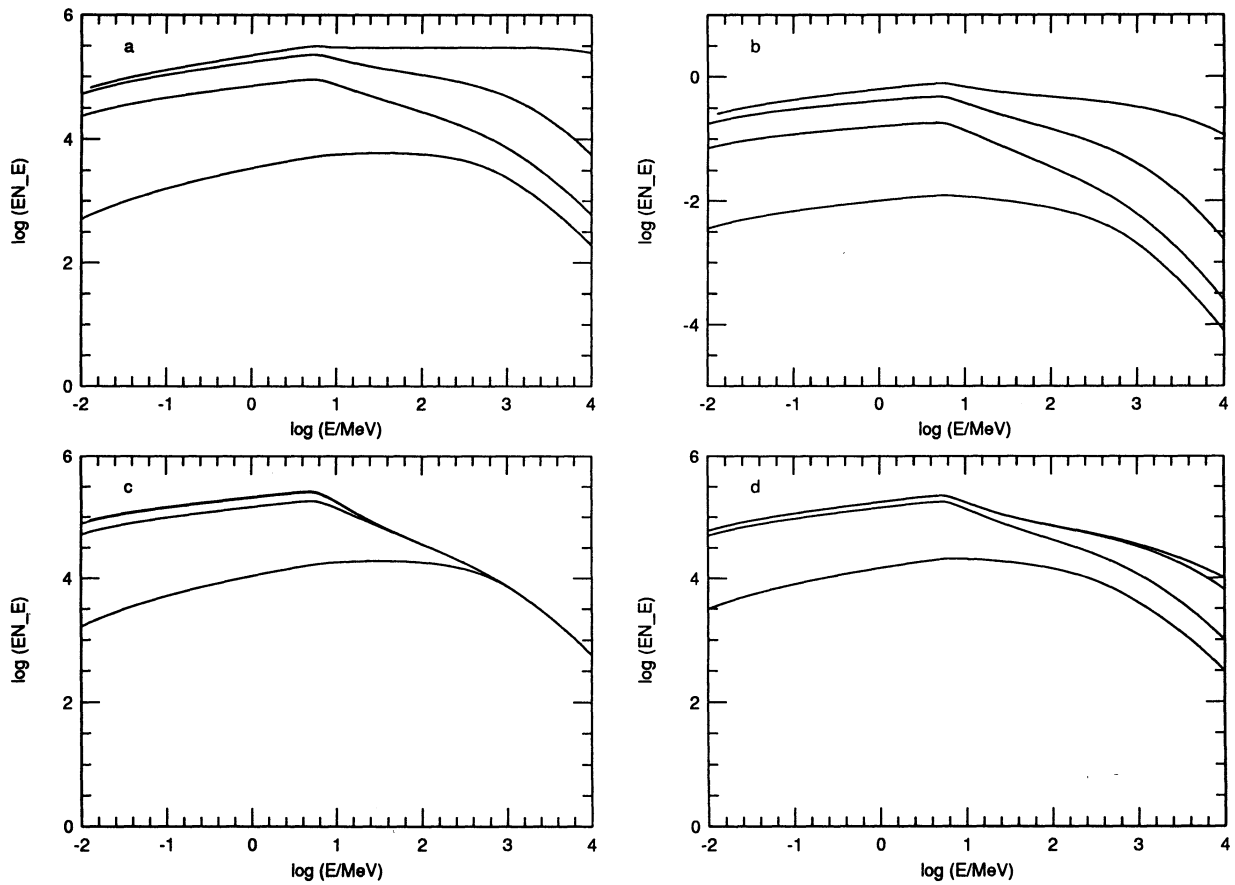

FIG. 2.—Local beamed photon spectra in the energy range 10 keV to 10 GeV. The different cases correspond to the cases presented in Fig. 1, respectively.

is being steadily accelerated within r_{ann}, e.g., by ponderomotive forces, so that Γ steadily increases. When Γ reaches $\Gamma_c \sim (m_e c^2/E_b)$, photons from near the upper cutoff in the X-ray spectrum can be scattered as γ-rays with energy $\sim \Gamma_c m_e c^2$. These same γ-rays will now create fresh pairs provided that $r \lesssim r_\gamma(\Gamma_c m_e c^2)$, which will increase the inertia of the jet and create a greater radiative drag on the outflow. In other words, there can be a positive feedback which will limit the jet Lorentz factor at a modest value $\Gamma \sim \Gamma_c$. Any tendency to increase the jet power is ultimately taken up in the form of more pairs and γ-rays as opposed to a greater energy per particle. The details of this limiting process depend upon the prescription for particle acceleration and the spectrum of the external radiation field. This will be discussed elsewhere.

It is also necessary to elucidate the jet Lorentz factor. Although it is possible for ultrarelativistic particles to stream with different speeds, a very small magnetic field strength suffices to keep the Larmor radii of the electrons and positrons at all energies of interest well below the size of the jet. This implies that there is, automatically, a local inertial frame in which the particle distribution function is, to good approximation, isotropic. This is the center of momentum frame of the particles. Now when the jet is particle energy dominated, then this will also define, to good approximation, the center of total momentum frame. If the jet energy density is predominantly electromagnetic, then the particle center of momentum frame will essentially be that in which the transverse electric field vanishes, at least on average; otherwise there will be an $\boldsymbol{E} \times \boldsymbol{B}$ drift along the jet. The speed of this frame can serve to define Γ in this case.

Now suppose that a jet has been collimated within an angle $\theta < \Gamma^{-1}$. The γ-rays scattered by the outflowing electrons will be beamed within an angle $\sim\Gamma^{-1}$ larger than the opening angle θ. As these γ-rays create pairs on the surrounding soft X-rays, they will quickly broaden the beam until $\theta \sim \Gamma^{-1}$. We can also argue that Γ^{-1} is likely to be an upper bound on the jet opening angle, because jets as we observe them on larger scale are continually being focused, possibly through the action of large-scale electromagnetic stress. Presumably, this is also occurring at radii smaller than those probed using VLBI, and so we suspect that this focusing will occur until $\theta \sim \Gamma^{-1}$. Even if this collimation does not take place, we can argue that there will effectively be several almost parallel jets causally disconnected and consequently kinematically independent and in general moving with different Lorentz factors. In this case, the observed flux for a given observer will usually be dominated by those parts of the jet for which the angle to the line of sight is $\sim\Gamma^{-1}$ and also is minimized subject to this condition. For jets with $\Gamma \gg \theta^{-1}$, we therefore need only consider those regions that are beamed toward us and, again, we can make the assumption that, at least locally, $\Gamma\theta \sim 1$. This does, however, open up the possibility that most of the power in relativistic jets may be essentially invisible to us.

4. DISCUSSION

This paper proposes that the hard X-ray emission observed from blazars is dominated by a beamed component, which is produced through inverse Compton scattering of seed soft photons by relativistic pairs accelerated in situ at the base of a γ-ray–emitting jet and which dominates the isotropic X-ray

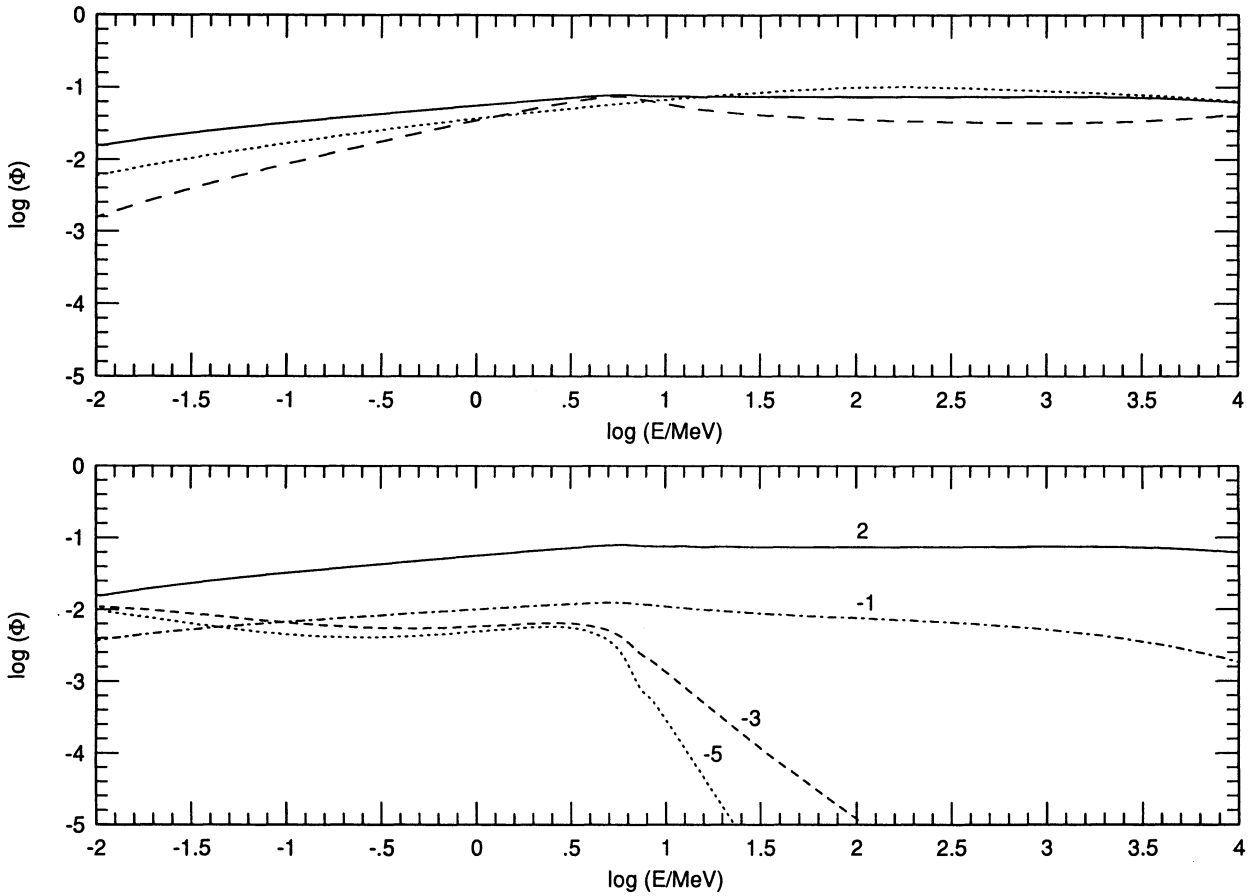

FIG. 3.—Emergent photon spectral efficiencies normalized to the total energy injected $\int \tilde{S}(E_e, r)dE_e dr$. *Upper panel:* $f(E_e) \propto \delta(E_e - E_{max})$ and standard soft photon spectrum (*solid line*), $g(E_e) \propto E_e^{-1.5}$ (*dotted line*), and $g(E_e) \propto E_e^{-0.5}$ (*dashed line*). *Bottom panel:* standard soft radiation spectrum and $f(E_e) \propto E_e^{\delta}$; δ labels the curves.

component that, we assert, is present in all AGNs. A similar scenario has been proposed previously, e.g., by Burns & Lovelace (1982), Dermer & Schlickeiser (1993), and Sikora et al. (1994). This view seems to be consistent with the rapid X-ray variability observed in several sources. The detection of uncorrelated flux variability at $\sim$20% level on a timescale of $\sim$2 days in the *ROSAT* hard (1.5–2.4 keV) and soft (0.1–0.3 keV) bands in 3C 273 (Leach, McHardy, & Papadakis 1995) suggests that the soft X-ray spectrum in this source is the extension of the "blue bump," whereas the hard component is produced in the jet. *Ginga* observations of the quasar 3C 279 indicate that the (2–20 keV) X-ray flux varied by $\sim$20% in less than an hour (Makino et al. 1989). Assuming that the X-ray emission is beamed, we find that the X-rays must originate from radii $< 10^{14}\ \Gamma^2$ cm, well within the γ-spheres of GeV γ-rays. The computed hard X-ray spectrum depends upon the distribution function of cascading pairs within the inner jet, which in turn depends on the spectrum of the isotropic UVX radiation. Unfortunately, the extreme UV spectrum is unknown, and this has a major influence on the hard X-rays. We find, however, that for plausible particle acceleration prescriptions and soft radiation spectra the model can reproduce the characteristic spectra observed typically in blazars.

In our model, the γ-ray spectral break reflects the high-energy cutoff in the isotropic X-ray spectrum, which is not observed directly in blazars because it is overwhelmed by the beamed emission from the jet. If the isotropic spectrum in blazars is similar to that observed in radio-quiet sources, then the relation between the break energy and the cutoff energy predicted by our model is roughly satisfied. The break near 100 MeV seen in the blazar 1633+382 (von Montigny et al. 1995) implies, according to our model, a cutoff at around 10 keV in the isotropic X-ray spectrum, which is atypical.

Observations of time variability at different wave bands may enable determination of the relative location of the emission regions. There is evidence for time lags between γ-ray flares and high-frequency radio flares observed in several blazars (Reich et al. 1993). In PKS 0528+134, for example, γ-ray high states observed by *CGRO* appear to precede the 37 GHz radio flare, which later propagated to lower frequencies, whereas γ-ray low states were measured during the decline of the 37 GHz outburst (Zhang et al. 1994). As argued qualitatively in Paper I, the γ-spheres at EGRET energies should be located well within the GHz radio core, and therefore time delays between γ-ray and radio variations are expected. Correlations between the millimeter/optical flux, that are most likely due to synchrotron emission, and the γ-ray flux which originates from roughly the same region, are also expected. In some sources (e.g., 3C 279) the synchrotron spectrum extends up to UV, and in some BL Lac objects it extends even to X-ray energies, whereas in other blazars (e.g., 3C 273) the optical to UV continuum is dominated by thermal emission, presumably associated with accretion onto the putative black hole. Recent multiwavelength observations of 3C 279 (Maraschi et al. 1994) indeed reveal

correlations between the optical-UV and γ-ray fluxes. The detection of a TeV outburst of duration of ~ 2 days in Mrk 421 by the Whipple Observatory (Kerrick et al. 1995), together with the nondetection of a significant change of the (0.1–10 GeV) flux by EGRET, which was observing the source simultaneously with Whipple, seems to be consistent with the view that the TeV γ-sphere is located well beyond the emission region (γ-spheres) of EGRET γ-rays (see Paper I). However, the origin of the X-ray flare detected by ASCA (Takahashi et al. 1994), which appears to be correlated with the TeV flare, is problematic. Quantitative calculations of the radius-frequency mapping are highly motivated and are currently underway (Levinson 1995). Simultaneous observations of the UV through the γ-ray flux may also provide a new way to probe energy dissipation in jets on the one hand, and the sub-parsec scale environment in AGNs on the other hand, and these are highly desirable.

We have neglected the contribution to the pair production opacity due the beamed hard X-rays themselves. This is a nonlinear process, like pair annihilation, which complicates the numerical analysis. This process may be important in cases in which the soft radiation spectrum cuts off at energies well below 100 keV, which is not very likely (many radio-quiet quasars, for example, exhibit hard X-ray spectrum extending to energies of order 100 keV or above), or in low-power BL Lac objects like Mrk 421, which are dominated by continuum emission. Otherwise, the neglect of this process appears to be justified (Paper I).

We have also attempted to relate to the X-ray cutoff E_b to the jet bulk Lorentz factor Γ by arguing that, under generic conditions of electromagnetic acceleration, $\Gamma \sim (m_e c^2/E_b)$. This, in turn, suggests a tentative observational test, namely that there may be a correlation between the measured superluminal speed in VLBI radio sources and the γ-ray break energy, as both of these should be inversely proportional to E_b. It is hoped that the present program of coordinated multiwaveband observations of γ-ray blazars will illuminate these issues.

We thank Ari Laor, Peter Michelson, and John Mattox for useful discussions. We thank the referee for clarifying the text. This work was supported by NASA grants NAGW 2816 and 2372 and NAG5 2504.

REFERENCES

Blandford, R. D. 1993, in Compton Gamma Ray Observatory, ed. N. Gehrels & M. Friedlander (New York: AIP), 533
Blandford, R. D., & Levinson, A. 1995, ApJ, 441, 79
Blom, J. J., et al. 1994, in Second Compton Symposium, ed. C. E. Fichtel, N. Gehrels, & J. P. Norris (New York: AIP), 644
Bloom, S. D., & Marscher, A. P. 1993, in Compton Gamma Ray Observatory, ed. N. Gehrels & M. Friedlander (New York: AIP), 578
Brunner, H., et al. 1994, A&A, in press
Burns, M. L., & Lovelace, R. V. E. 1982, ApJ, 262, 87
Collmar, W., et al. 1993, in Compton Gamma Ray Observatory, ed. N. Gehrels & M. Friedlander (New York: AIP), 484
———. 1994, in Second Compton Symposium, ed. C. E. Fichtel, N. Gehrels, & J. P. Norris (New York: AIP)
Dermer, C., & Schlickeiser, R. 1993, ApJS, 416, 458
Ghisellini, G., & Maraschi, L. 1989, ApJ, 340, 181
Kennel, C. F., & Coroniti, F. V. 1984, ApJ, 283, 710
Kerrick, A. D., et al. 1995, ApJ, 438, L59
Königl, A. 1981, ApJ, 243, 700
Kurfess, J. D., et al. 1994, in IAU Symp. 159, Active Galactic Nuclei across the Electromagnetic Spectrum, ed. A. Blecha & T. Courvoisier (Dordrecht: Kluwer), 39
Laor, A., et al. 1994, ApJ, 435, 611
Leach, C. M., McHardy, I. M., & Papadakis, I. E. 1995, MNRAS, in press
Levinson, A. 1995, ApJ, submitted
Lichti, G., et al. 1994, in Second Compton Symposium, ed. C. E. Fichtel, N. Gehrels, & J. P. Norris (New York: AIP), 611
Makino, F., et al. 1989, ApJ, 347, L9
Maraschi, L., et al. 1994, ApJ, 435, L91
Melia, F., & Königl, A, 1989, ApJ, 340, 162
Orr, M. J. L., & Browne, I. W. A. 1982, MNRAS, 200, 1067
Reich, W., et al. 1993, A&A, 273, 65
Sikora, M., Begelman, M., & Rees, M. 1994, ApJ, 421, 153
Svensson, R. 1987, MNRAS, 227, 403
Takahashi, T., et al. 1994, IAU Circ., No. 5993
Thompson, D. J., et al. 1994, in IAU Symp. 159, Active Galactic Nuclei across the Electromagnetic Spectrum, ed. A. Blecha & T. Courvoisier (Dordrecht: Kluwer), 49
Vermeulen, R. C., & Cohen, M. H. 1994, ApJ, 430, 467
von Montigny, C., et al. 1995, ApJ, 440, 525
Wilkes, B. J., & Elvis, M. 1987, ApJ, 323, 243
Zdziarski, A. 1988, ApJ, 335, 786
Zhang, Y. F., et al. 1994, ApJ, 432, 91